

SDSS J131339.98+515128.3: A new gravitationally lensed quasar selected based on near-infrared excess

Eran O. Ofek^{*1}, Masamune Oguri², Neal Jackson³, Naohisa Inada⁴, and Issha Kayo⁵

¹ *Division of Physics, Mathematics and Astronomy, California Institute of Technology, Pasadena, CA 91125*

² *Kavli Institute for Particle Astrophysics and Cosmology, Stanford University, Menlo Park, CA 94025.*

³ *The University of Manchester, Jodrell Bank Observatory, Macclesfield, Cheshire SK11 9DL, UK.*

⁴ *Cosmic Radiation Laboratory, RIKEN (The Institute of Physical and Chemical Research), 2-1 Hirosawa, Wako, Saitama 351-0198, Japan.*

⁵ *Department of Physics and Astrophysics, Nagoya University, Chikusa-ku, Nagoya 464-8602, Japan*

Accepted ? Received ? in original form ?

ABSTRACT

We report the discovery of a new gravitationally lensed quasar, SDSS J131339.98+515128.3, at a redshift of 1.875 with an image separation of $1''.24$. The lensing galaxy is clearly detected in visible-light follow-up observations. We also identify three absorption-line doublets in the spectra of the lensed quasar images, from which we measure the lens redshift to be 0.194. Like several other known lenses, the lensed quasar images have different continuum slopes. This difference is probably the result of reddening and microlensing in the lensing galaxy. The lensed quasar was selected by correlating Sloan Digital Sky Survey (SDSS) spectroscopic quasars with Two Micron All Sky Survey (2MASS) sources and choosing quasars that show near-infrared (IR) excess. The near-IR excess can originate, for example, from the contribution of the lensing galaxy at near-IR wavelengths. We show that the near-IR excess technique is indeed an efficient method to identify lensed systems from a large sample of quasars.

Key words: gravitational lensing — quasars: individual (SDSS J131339.98+515128.3)

1 INTRODUCTION

Construction of large samples of gravitational lenses has been shown to be a unique tool for studying galaxy mass profiles (e.g., Cohn et al. 2001; Rusin et al. 2002; Koopmans & Treu 2003; Rusin & Kochanek 2005; Treu et al. 2006), galaxy evolution (e.g., Kochanek et al. 2000; Ofek et al. 2003; Treu & Koopmans 2004; Rusin & Kochanek 2005), and cosmology (e.g., Linder 2004; Oguri 2007). Moreover, individual lenses enable us to study the lensed quasar engine (e.g., Kochanek et al. 2007) and the dark matter content of galaxies through microlensing (e.g., Wambsganss et al. 2000; Schechter & Wambsganss 2002).

The photometric and spectroscopic quasar samples of the Sloan Digital Sky Survey (SDSS; York et al. 2000) were estimated to contain ~ 1000 lensed quasars. However, in practice, because of seeing limitations, it is challenging to find most of these lenses. The most successful search for lensed quasars in the SDSS (Oguri et al. 2006) utilizes the morphological properties of SDSS quasars, as well as colours of nearby objects, to efficiently select lensed quasars with

image separation greater than $1''$ and flux ratio above ~ 0.3 . Lensed quasars can also be discovered spectroscopically by looking for a compound spectrum consisting of a galaxy and a quasar (e.g., Johnston 2003). Since these techniques locate only a fraction of lensed quasars in the SDSS, it is of great importance to develop additional approaches in order to find more lenses, especially lenses with image separation below $\sim 1''$.

The efficiency of lens surveys can be enhanced by combining multi-wavelength data. For instance, Kochanek et al. (1999) compared optical and radio properties of wide-separation quasar pairs to argue that they are binary quasars rather than gravitational lenses. Jackson & Browne (2007) proposed a lens search method that exploits the small position differences between radio positions of lensed images and optical positions of lensing galaxies. The method may enhance the efficiency of lens searches by up to a factor of ~ 10 . Another approach, presented by Haarsma et al. (2005), is to look for extended radio lobes which are lensed by galaxies along the line of sight. We note that the magnification bias for such multi-wavelength surveys is more complicated than usual (e.g., Borgeest et al. 1991; Ofek et al. 2002; Wytithe et al. 2003).

* e-mail: eran@astro.caltech.edu

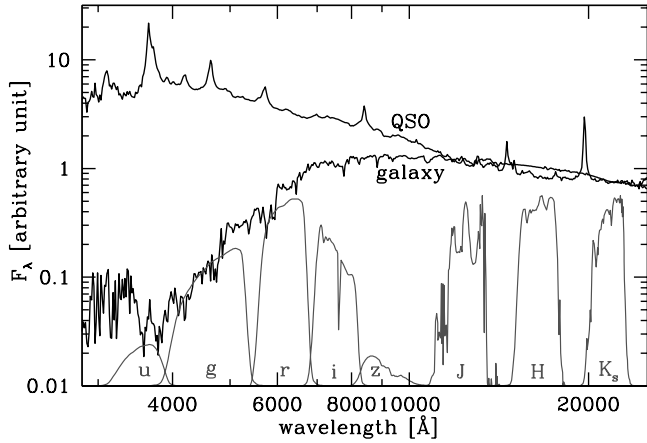


Figure 1. Illustration of the spectra of an elliptical galaxy (Mannucci et al. 2001) at a redshift of 0.5 and a quasar (Vanden Berk et al. 2001) at a redshift of 2.0. The spectra are normalized such that the i -band magnitude difference is $i_{\text{gal}} - i_{\text{QSO}} = 1$, which is typical for lensed quasar systems. The transmission curves of the SDSS $ugriz$ and the 2MASS JHK_s filters are also shown (Moro & Munari 2000).

In this paper we present an approach for finding lensed quasars in the SDSS data. This method relies on selecting, as candidate lens systems, quasars with near-IR excess, which may be due to the contribution of a lensing galaxy. We note in this context that Gregg et al. (2002) suggested that red quasar samples may contain a large number of lensed quasars due to reddening by the lensing galaxy. We show that the quasar SDSS J131339.98 + 515128.3 selected by this method is a new gravitationally lensed quasar, which is confirmed from imaging and spectroscopic follow-up observations.

The outline of this paper is as follows. We describe the near-IR excess selection method and the lensed quasar candidates in §2. In §3 we present the observations of the new lens we have found, and its spectroscopy and photometry are described in §4. We model the new system in §5 and discuss the results in §6. Finally the conclusions are given in §7.

2 SELECTION OF LENSED QUASAR CANDIDATES BASED ON THE NEAR-IR EXCESS METHOD

The selection process for gravitational lenses presented here is based on the fact that most lenses are red galaxies whereas quasars are much bluer. Therefore, even if the flux from the lens galaxy does not dominate at visible-light frequencies, which is quite common among lens systems discovered to date, it is expected that in some cases the lensing galaxy has a non-negligible contribution to the integrated brightness of the lens system at near-IR frequencies. This suggests that some of the lens systems may be characterized by a near-IR excess that originates from the lensing galaxy. Figure 1 illustrates this idea by showing template spectra of quasars and early-type galaxies redshifted to typical source and lens redshifts, respectively. This plot clearly indicates that the lensing galaxy can modify the near-IR to visible light colour

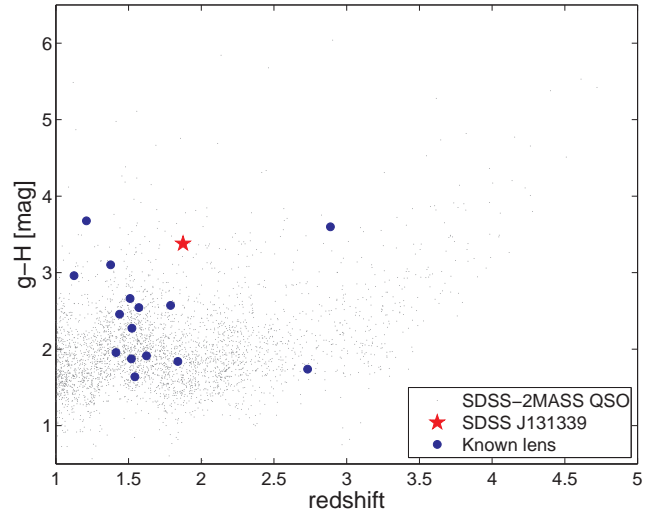


Figure 2. The optical-IR colour $g - H$ versus redshift for 3347 ($= 3132 + 215$) SDSS-2MASS quasars (dots) with SDSS measured redshifts above 1, redshift confidence $> 90\%$, $i < 19.0$ mag, and angular distance between the SDSS and 2MASS sources smaller than $1''.5$. Also shown are the positions of known lensed quasars (filled circles) and of SDSS J131339.98 + 515128.3 (pentagram).

of lensed quasar systems. In this paper, we adopt the $g - H$ colour as a measure of the near-IR excess.

In order to exploit this idea to look for new lensed quasars in the SDSS, we cross-correlated the SDSS Data Release 5 (DR5) spectroscopic quasars[†] with the Two Micron All Sky Survey (2MASS) point sources (Cutri et al. 2003). Specifically we looked for a 2MASS point source within $5''$ from each quasar position and extract its IR magnitudes[‡]. For our lens search, we have constructed a subsample of candidates by selecting quasars with: redshift $3 > z > 1$; redshift confidence $z_{\text{conf}} > 0.9$; i -band magnitude brighter than 19.0; and angular distance between the SDSS and 2MASS sources smaller than $1''.5$. We excluded low-redshift quasars because their fluxes are sometimes affected to a large extent by contributions from host galaxies. We also avoided selecting high redshift quasars since the lens galaxies of such quasars will be typically at high redshifts, and therefore are too faint to be detected in the 2MASS survey (see §6.2). The smaller angular distance cutoff (i.e., $1''.5$) selects 95% of all the SDSS-2MASS sources found up to $5''$ apart. We use the relatively small offset in order to remove well separated quasar-galaxy pairs. The resulting number of SDSS-2MASS quasars is 3132. In Figures 2 and 3 we show the locations (dots) of the 3132 SDSS-2MASS quasars passing these selection criteria, in addition to 215 quasars found above redshift 3, in the redshift versus $g - H$ colour and $g - r$ versus $g - H$ colour phase spaces, respectively. Also shown are the

[†] In this paper we do not use the DR5 quasar catalog of Schneider et al. (2007), because this work began before the public release of their catalog.

[‡] We make this catalog available to the community through the Vizier service: <http://vizier.u-strasbg.fr/cgi-bin/VizieR>. The online catalog includes also cross correlation with the FIRST radio catalog (Becker et al. 1995).

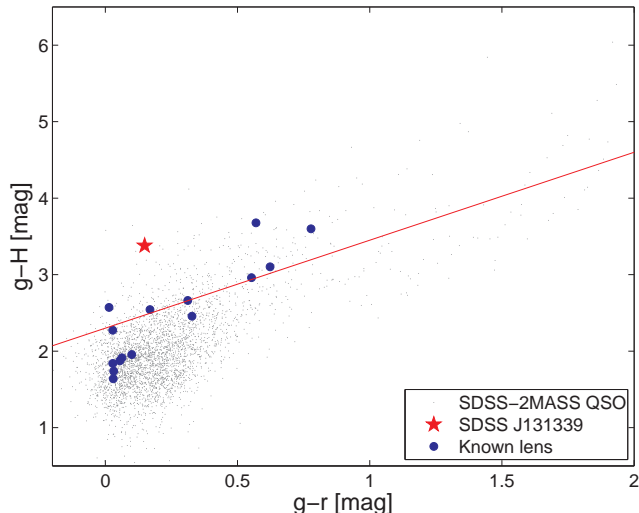


Figure 3. Same as Figure 2, but for $g - H$ versus $g - r$. The line marks our selection cut in this colour space (see text).

positions of known lensed quasars with SDSS and 2MASS detections (filled circles), and the position of the new lens reported in this paper (SDSS J131339.98+515128.3; pentagram). Figure 3 indicates that the optical-IR colour $g - H$ is correlated with the optical colour $g - r$, reflecting the fact that the quasar spectral energy distributions are characterized by a power-law. The Figure suggests that known lenses tend to be redder than the “average” quasar.

In order to test the feasibility of this method, from the 3132 quasars, we selected objects whose colours satisfy: $g - H > 1.15(g - r) + 2.3$ (above the line in Figure 3), where, g and r are the g and r -band magnitudes corrected for Galactic extinction (Schlegel et al. 1998; Cardelli et al. 1989). This colour cutoff is arbitrary and does not rely on any quantitative argument. We choose this cut as an initial trial to study the feasibility and efficiency of the near-IR-excess lensed quasar selection method. Using the $g - H$ cut we selected 294 quasars, of which the following 7 are previously known lenses: HS0810+2554 (Reimers et al. 2002); SBS0909+523 (Kochanek et al. 1997; Oscoz et al. 1997); SDSS J1155+6346 (Pindor et al. 2004); SDSS J1206+4332 (Oguri et al. 2005); SDSS J1226-0006 (Inada et al. in preparation); SDSS J1335+0118 (Oguri et al. 2004); SDSS J1524+4409 (Oguri et al., in preparation). Therefore the lens search efficiency is already $> 2\%$ at this point, before introducing any morphological constraints.

We make the lens survey more efficient, and reduce the number of targets for follow up observations, by applying a simple cut on the morphology of the quasars, in the same spirit as Oguri et al. (2006). Specifically, we set the condition that the SDSS stellar likelihood of the candidates is smaller than 0.1 in both the r and i -bands. The low stellar likelihood of < 0.1 means that the object is poorly fitted by the point spread function (PSF). We note that the completeness for including extended quasars in the spectroscopic quasar sample begins to decrease at $z = 2.2$, and at $z \gtrsim 3$ most extended quasars are not targeted (Oguri et al. 2006). We finally compiled a list of 56 candidates that survived the morphology cut (14 of them with $z > 2.2$). We note that all

the 7 previously known lenses pass the colour and morphological criteria. Therefore, the lens selection efficiency improves to more than 10%.

Next, we look for new gravitationally lensed quasars in this list of candidates. We exclude seven of the radio-loud targets in the list, because they were observed at $0''.22$ resolution in the CLASS radio lens survey and confirmed not to be lenses (e.g., Myers et al. 2003). We observed two targets at the Subaru 8.2 m telescope and 12 targets at the University of Hawaii 2.2 m telescope, and found that one of the targets, SDSS J131339.98 + 515128.3, consists of two optical point sources and an extended source, making it an excellent lens candidate. SDSS J131339.98 + 515128.3 has no detectable radio flux at the ~ 1 mJy limit of the FIRST 20-cm survey (Becker et al. 1995).

3 OBSERVATIONS OF SDSS J131339.98+515128.3

On UTC 2007 April 12.95, we observed our lens candidate SDSS J131339.98+515128.3 with the Tektronix 2048 \times 2048 CCD camera (Tek2k) at the University of Hawaii 2.2 m telescope, in VRI -bands. The exposure time was 300 s for each band. The frames with a pixel scale of $0''.2195 \text{ pix}^{-1}$, were obtained under seeing of about $0''.8$, and are shown in Figure 4. The data were reduced using standard IRAF[§] tasks, and photometric calibration was performed using observations of the Landolt (1992) standard star fields PG0918+029 and PG1633+099.

On UTC 2007 March 10.56 we obtained a 1400 s spectrum of SDSS J131339.98 + 515128.3 using the Low Resolution Imaging Spectrometer (LRIS; Oke et al. 1995) on the Keck-I 10 m telescope. In the red arm we used the 400/8500 grating, and on the blue side we used the 400/3400 grism. The spectrum was obtained using the $0''.7$ slit, at a position angle of 16° , which goes through the two lensed quasar images. For flux calibration we observed the spectrophotometric standard star HZ 44. The spectra were reduced using tools developed in the MATLAB environment (Ofek et al. 2006).

4 PHOTOMETRY AND SPECTRA

The positions and magnitudes of the lensed quasar images and lensing galaxy are derived by fitting the system with two PSFs and a galaxy profile using Galfit (Peng et al. 2002). We first model the galaxy by a Sersic profile and found the best-fit Sersic index to be $n \approx 4$. Therefore, we fix the index to $n = 4$, a typical value for early type galaxies, to compute the relative positions and magnitudes. Tables 1 and 2 summarize the fit results. The separation of the lensed quasar images is $1''.24$, and the flux ratios between the two quasar images

[§] The Image Reduction and Analysis Facility (IRAF), is general purpose software system for the reduction and analysis of astronomical data. IRAF was written by the programming group at the National Optical Astronomy Observatories (NOAO) in Tucson, Arizona. NOAO is operated by the Association of Universities for Research in Astronomy (AURA), Inc. under cooperative agreement with the National Science Foundation

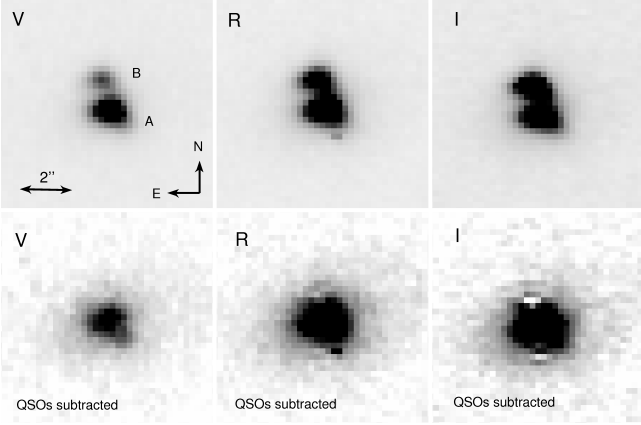


Figure 4. Upper panels: *VRI* frames (from left to right) around SDSS J131339.98 + 515128.3, obtained at the University of Hawaii 2.2 m telescope. The frames are presented with the same gray-scale stretch, and the colour difference between the two quasar images is apparent. Throughout this paper the brighter quasar image (south) is denoted A and the fainter (north) is denoted B. Lower panels: *VRI* frames (from left to right) of the lensed system after subtracting the two quasar images. The lensing galaxy is clearly detected. The frames are displayed with the same gray-scale stretch, which is about 1/6 of the gray-scale stretch in the upper panels. The white dots are residuals due to the subtraction of the lensed quasar images.

Object	$\Delta\alpha$ [arcsec.]	$\Delta\delta$ [arcsec.]
A	0.0	0.0
B	-0.325 ± 0.002	1.193 ± 0.002
G	-0.064 ± 0.009	0.153 ± 0.009

Table 1. The relative positions were calculated from the mean of the *VRI* image positions and the errors were estimated from the scatter. The absolute position of image A is: 13:13:39.98 +51:52:28.37 (J2000.0).

are 3.63, 1.67 and 0.92 in the *VRI*-bands, respectively. We note that the lensing galaxy is also apparent in an *R*-band image taken using the Suprime-cam on the Subaru telescope (Miyazaki et al. 2002), which was retrieved from the Subaru telescope archive (Baba et al. 2002). However we did not use the Subaru data for our analysis because the PSF of the image is very unusual, which prevents reliable photometry and astrometry of the system.

Object	<i>V</i> [mag]	<i>R</i> [mag]	<i>I</i> [mag]	<i>b/a</i>	PA [deg]	R_e [arcsec.]
A	18.26	18.09	17.45			
B	19.66	18.65	17.36			
G	18.74	18.23	17.49	0.78	-71	0.75

Table 2. The *VRI* magnitudes of the lensed quasar images and the lensing galaxy as obtained by two PSFs+galaxy fitting. The magnitudes are given in the Vega system. We fitted a Sersic profile to the galaxy using Galfit (Peng et al. 2002). The best fit Sersic index is ~ 4 . R_e is the effective radius of the galaxy.

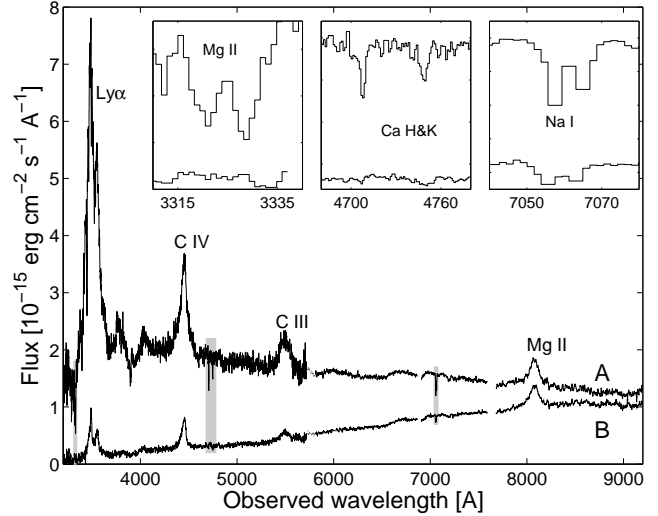


Figure 5. The spectra of SDSS J131339.98 + 515128.3 images A (upper spectrum) and B (lower spectrum). The three insets show absorption lines of Mg II ($\lambda\lambda 2798.1-2802.7 \text{ \AA}$), Ca II ($\lambda\lambda 3934.8-3969.6 \text{ \AA}$), and Na I ($\lambda\lambda 5889.9-5895.9 \text{ \AA}$), in the spectra, presumably due to the lensing galaxy (see Figure 4). The gray boxes mark the position of the insets in the spectrum. The gaps in the spectra are due to removal of telluric absorption lines.

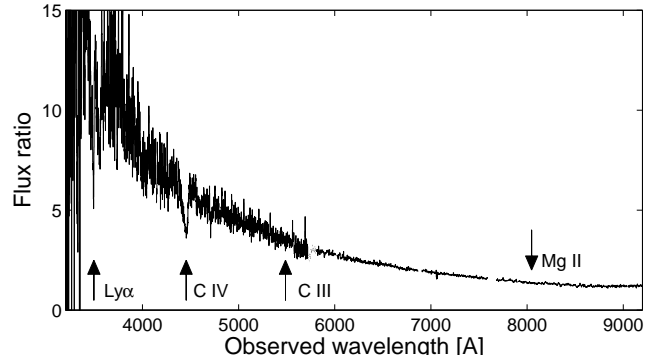


Figure 6. The ratio between the spectra of SDSS J131339.98 + 515128.3 images A and B. The positions of the quasar broad emission lines are marked by arrows.

The spectra of the two images of SDSS J131339.98 + 515128.3 are displayed in Fig 5, and the flux ratio, as a function of wavelength, between the spectra of images A and B is presented in Fig. 6. The two quasars, marked by A and B, have identical redshifts with similar (though not identical) broad emission lines, but markedly different continua. We will discuss the possible origins of this large colour difference in §6. In the spectra we detect three absorption doublets of Mg II, Ca II and Na I (insets in Figure 5) at a redshift of 0.194 ± 0.005 , which are probably induced by the lensing galaxy. Additional support for this interpretation comes from the fact that the stellar absorption features of Ca H&K are stronger for image A, which is closer to the lensing galaxy.

We fitted the Galactic extinction (Schlegel et al. 1998) corrected colours of the galaxy with synthetic photometry of galaxy spectral templates (Kinney et al. 1996) assuming the lens redshift of 0.194. The visible-light colours of the

lensing galaxy are best fit with a late-type galaxy. However, these colours may be affected by the light of image A, which is only $0''.17$ from the position of the galaxy. The late-type galaxy colours may contradict the best-fit Sersic index of ~ 4 . To explore this issue, we tried fitting the lens galaxy with an $n = 1$ Sersic profile, and found that the fit to the imaging data is reasonable. Therefore, further observations are needed for a more conclusive classification of the lensing galaxy.

5 LENS MODELING

We fitted, in the source plane, the image positions with an elliptical softened power law mass model (Barkana 1998). In the fit we assumed a core radius of 1 milliarcsecond (mas) and used the following priors: the lens position to lie within 27 mas from the galaxy center (about 3 times the errors in the galaxy position); the lens eccentricity to be less than 0.35; the position angle (PA) to lie between -40 and -100 deg (which is ~ 30 deg from the PA of the galaxy light distribution); and the power-law of the two-dimensional mass distribution, α , to be 1.0 (corresponding to an isothermal sphere). The best fit parameters are: centre-of-mass position $\Delta R.A. = -0''.048$, $\Delta Dec. = 0''.175$ (relative to image A); eccentricity 0.16; PA = -70 deg; and the position of the source is $\Delta R.A. = -0''.163$, $\Delta Dec. = 0''.595$. The time delay, estimated using the analytic formula for an isothermal potential (Kassiola & Kovner 1993), is around 30 days, assuming the third year WMAP cosmology[¶] (Spergel et al. 2007).

Given these parameters, the derived magnifications are -0.4 and 2.5 for images A and B, respectively. These predicted macro-model magnifications are inconsistent with the observed flux ratio (i.e., the nearest image to the lens is the brightest), and this discrepancy is discussed in the next section.

6 DISCUSSION

Here we discuss the efficiency of our near-IR excess method (§6.1), its selection effects (§6.2), as well as the nature of the different colours of the lensed images of SDSS J131339.98 + 515128.3 (§6.3).

6.1 Efficiency of the near-IR excess method

Our preliminary selection criteria in the $g - r$ versus $g - H$ colour space selected 294 candidates, of which at least 8 are gravitational lenses. The efficiency $\geq 8/294 \sim 3\%$ is apparently higher than lensing rates in quasar samples. For comparison, the lensing efficiency of the CLASS lens survey was $\sim 0.14\%$ (Browne et al. 2003), and about 1% in the Hubble Space Telescope snapshot survey (e.g., Maoz et al. 1993). Therefore we conclude that our near-IR excess cut indeed enhances the fraction of lenses in the sample. After the introduction of the morphology selection criterion, the

efficiency boosts to $\geq 8/56 \sim 14\%$. However, such a morphology cut may drop very small separation lensed quasars that are barely resolved in the SDSS.

We expect the efficiency of this method to increase for intrinsically fainter quasars in which the lensing galaxy has a higher probability of dominating the system light. We comment that a significant fraction of false positive candidates in our near-IR excess sample are close pairs of quasars and galaxies which are inevitably selected given the philosophy of the method.

6.2 Selection effects of the near-IR excess method

The near-IR excess selection method is biased toward systems in which the lensing galaxy is apparently bright, and therefore, on average at lower redshift than the typical redshift of lensing galaxies. Moreover, these systems will have larger than average image separations. This is a consequence of the fact that a brighter, and hence more massive, lensing galaxy implies a larger image separation. The lower lens redshift also results in larger image separation. Therefore, caution is needed when using lens systems found by such a method in analysis which requires lensed quasar samples with non-biased lens redshift distribution (e.g., Kochanek 1992; Ofek et al. 2003; Capelo & Natarajan 2007).

In addition, this method will probably be biased toward detecting doubly imaged lensed quasars in which the average magnification is smaller than in quadruply lensed systems, and therefore, the lensing galaxy has a higher probability to dominate the total light in the near-IR. We note that in a red-band flux-limited sample, like the one we use here (i.e., $i < 19$ mag), the incidence of lenses will be increased due to the contribution of the lens galaxy to the total system light, relative to a sample which is not flux limited.

The images of some lensed quasars show remarkable rest-frame UV continuum differences (e.g., HE1104–1805 Wisotzki et al. 1993) that are variable with time (e.g., Ofek & Maoz 2003; Poindexter et al. 2007). Such continuum differences can make them appear redder. Although this type of lensed quasars is relatively rare, it is possible that the new quasar presented in this paper belongs to this group. Furthermore, it is well known that narrow and broad absorption line QSOs are redder than typical quasars (e.g., Brotherton et al. 2001), and this is especially true for radio selected quasars (e.g., Menou et al. 2001). Therefore, the near-IR excess method may be efficient for looking for lensed broad absorption line quasars, which may be useful for probing the structure of quasar outflows using microlensing (Chelouche 2005).

Gregg et al. (2002) argued that the population of very red quasars contains a large fraction of gravitational lenses because of reddening by the lensing galaxies. Although we compare optical-IR colours ($g - H$) of quasars with the optical ($g - r$) colours in order to distinguish between red/reddened quasars and lensed quasar systems, it is still possible that this method is biased toward selecting red lensed quasars. This is also suggested by the fact that one of the lensed components of our new lens has a red colour. Note, however, that highly extinguished lenses are relatively rare (e.g., Falco et al. 1999).

Finally, we note that a basic limitation of this approach is that it can detect the lensing galaxy only if it is brighter

[¶] $H_0 = 70.4 \text{ km s}^{-1} \text{ Mpc}^{-1}$; $\Omega_m = 0.27$; $\Omega_\Lambda = 0.73$.

than the limiting magnitude of the near-IR survey that is being used. In particular it should be emphasized that the current use of this method is limited by the shallow detection limit of the 2MASS survey used here. In the 2MASS survey $5L_*$ galaxies can be detected up to a redshift of ~ 0.2 . Thus, lensed systems with higher-redshift lensing galaxies cannot be efficiently detected using this method. However, future surveys (e.g., UKIDSS, Lawrence et al. 2006; WISE, Mainzer et al. 2005) can be used to select lensing galaxies to redshifts up to ~ 1.0 , making the near-IR excess method much more useful.

6.3 The origin of the different colours of the lensed images

The lensed images of SDSS J131339.98 + 515128.3 are distinctly different in their spectral continuum slopes, but the shapes and equivalent widths of their broad emission lines are similar (though not identical). Such colour differences are not common among lensed quasars, although there are several known examples (e.g., HE1104–1805). Two obvious possibilities are that the different colours are caused by microlensing, or/and by extinction and reddening in the lensing galaxy (e.g., Falco et al. 1999; Elíasdóttir et al. 2006).

The equivalent widths of the Na I absorption lines in the spectra of images A and B (Figure 5), are $\sim 2.5 \text{ \AA}$ and $\sim 1.5 \text{ \AA}$, respectively. The known correlation between Na I absorption lines and extinction (e.g., Turatto et al. 2003) suggests that the lensed quasar images are extinguished with E_{B-V} in the range of 0.1 to 1 mag.

To estimate the relative extinction between the two quasar images, we divided the continuum-subtracted spectrum of image A by that of image B (i.e., we used only the broad line flux), and fit it with extinction curves (Cardelli et al. 1989). The best fit extinction we have found is $E_{B-V} = 0.5 \text{ mag}$ (assuming $R_V = 3.08$). Next, we divided the spectrum of image A by the de-reddened spectrum of image B (i.e., $E_{B-V} = 0.5 \text{ mag}$, $R_V = 3.08$). The result is roughly consistent with a power-law, $\sim \lambda^{-1 \pm 0.1}$. This indicates that extinction alone probably cannot explain the entire difference between the spectra. We note that if we use the entire spectra (continuum and lines) to fit for a relative extinction curve between the two lensed images, a reasonable fit is found with $E_{B-V} \approx 0.7 \text{ mag}$. However, this does not constitute a perfect fit, and the residuals between the spectra are not monotonic with wavelength, which is difficult to explain.

Contrary to extinction, we expect microlensing to alter the spectral continuum of a quasar image, but keep the broad emission lines unchanged. The reason for this is that the approximate length scale over which microlensing effects are expected to average out, is several times the microlensing Einstein radius. The expected Einstein radius for $1 M_\odot$ microlensing in this system is about 0.03 pc (in the source plane), which is of the same order of magnitude as the expected size of the accretion disks of bright quasars.

Interestingly, as shown in Fig 6, the ratio between the lensed images' broad emission lines is not identical to the ratio of the continua around these lines. This can be investigated further by a detailed comparison of the line profiles, shown in Fig. 7. Here we have made the assumption that the relative reddening between images A and B is $E_{B-V} = 0.5 \text{ mag}$. Then, for each broad emission line, we

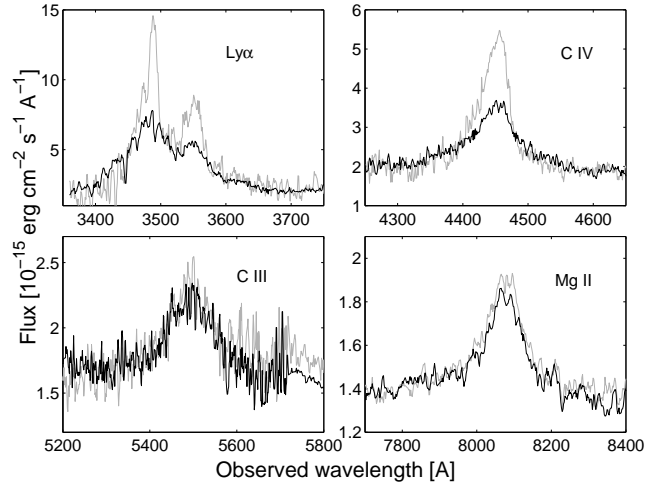


Figure 7. Each panel shows one of the major emission lines in the spectrum: Ly α , C IV, C III] and Mg II, at the observed wavelengths. In each case, the black-line shows the spectrum of image A, and the gray line represents the observed, extinction corrected ($E_{B-V} = 0.5$, $R_V = 3.08$), spectrum of image B, multiplied by 1.5, 1.0, 0.93 and 0.64, for the Ly α , C IV, C III], and Mg II, respectively. It can be seen that this scaling gives a good overlap for Mg II and C III] lines, and for the broad components of the other lines, but that there are narrow components in Ly α and C IV lines, which do not overlap well, being considerably greater in image B.

have multiplied the de-reddened spectrum of image B by a wavelength dependent factor, in order to match the continua of images A and B around these lines. As shown in Fig. 7, we find remarkably good agreement between the lines of images A (black) and B (gray), in the case of the C III] and Mg II lines. In the other two lines (Ly α and C IV) the broad wings of the line also agree, but there is clearly a narrower component present within the broad emission lines of image B that is absent in image A.

There are two possible explanations for this result. The first is that the broader component of the emission lines originates in a region small enough to be microlensed, together with the optical continuum, in the sense that both continuum and broad component of the emission lines in image B are suppressed. We note that microlensing of a quasar's broad emission lines was probably detected in SDSS 1004+4112 (Richards et al. 2004). The second possibility is that reddening is mainly responsible for this difference. In this case we would require that the continuum and broad line components are affected by a different degree of reddening than the narrow component of the emission lines. In order for extinction in the lensing galaxy to produce a differential effect of this type, it should be patchy on a length scale of the broad-line region size (i.e., $\sim 1 \text{ pc}$).

The most simple explanation for the spectral differences between the lensed quasar images, is that while they are affected by extinction, microlensing plays a significant role. The spectral differences, after applying a relative extinction of $E_{B-V} = 0.5 \text{ mag}$ between the images, suggests that the quasar region responsible for the short-wavelength ($\lambda_{rest} \sim 1400 \text{ \AA}$) continuum emission is more magnified than the region emitting the longer-wavelength ($\lambda_{rest} \sim 2800 \text{ \AA}$) radiation. Indeed, this is consistent with what is expected from

microlensing of a quasar accretion disk. Moreover, the negative parity image (image A in our case) has a higher probability of being magnified by microlensing relative to the positive parity image (image B; Schechter & Wambsganss 2002; Mortonson et al. 2005). Indeed, contrary to the macro-model (§5) prediction, image A is magnified relative to image B. Probably the best way to verify that microlensing is responsible for some of the spectral differences between the lensed images, is to look for temporal colour changes between the two lensed images, similar to the colour variability observed in HE1104–1805 (Poindexter et al. 2007).

7 CONCLUSION

Given the promising future of whole sky surveys (e.g., SkyMapper, Keller et al. 2007; PanSTARR, Kaiser et al. 2005; LSST, Tyson 2005), a variety of methods to search for gravitationally lensed quasars are needed. One possibility, suggested by Kochanek et al. (2006), is to look for variable sources that are extended, presumably due to lensed quasar images and/or lensing galaxy. However, this method, like the SDSS quasar lens search (Oguri et al. 2006), is limited by the seeing of ground based telescopes.

We have proposed that some classes of lensed quasars can be identified efficiently by looking for single-epoch near-IR excess of known (spectroscopic or photometric) quasars. The near-IR method is based on the fact that at least some lensed quasar systems will be redder due to the presence of a bright lensing galaxy (e.g., Fig 1). The use of the near-IR excess method is demonstrated by our discovery of the new lensed quasar SDSS J131339.98 + 515128.3. Follow up observations have shown it to be a doubly-imaged lensed quasar, at $z = 1.875$, with an image separation of $1''.24$. We also identified the lensing galaxy at a redshift of 0.194. The continua of the lensed quasar images are markedly different, presumably due to extinction and microlensing effects. The discovery of the new lens as well as the presence of many known lensed quasars in the near-IR excess lens candidates sample suggests that the near-IR excess is indeed an efficient way to select lensed quasar systems from large samples of quasars.

ACKNOWLEDGMENTS

EOO, MO, and NJ would like to thank the Kavli Institute for Theoretical Physics and the organizers of the KITP workshop “Applications of Gravitational Lensing: Unique insights into Galaxy Formation and Evolution” for their hospitality; this work was initiated at this KITP workshop. It is a pleasure to thank the referee, Chris Kochanek, for useful comments on the manuscript. This research was supported in part by the National Science Foundation under Grant No. PHY05-51164, and also by Department of Energy contract DE-AC02-76SF00515 and by the European Community’s Sixth Framework Marie Curie Research Training Network Programme contract no. MRTN-CT-2004-505183 “ANGLES”. Use of the UH 2.2-m telescope for the observations is supported by NAOJ. Based in part on data collected at Subaru telescope and obtained from the SMOKA archive, which is operated by the Astronomy Data Center, National

Astronomical Observatory of Japan. NI acknowledges support from the Special Postdoctoral Researcher Program of RIKEN.

REFERENCES

- Baba, H., et al. 2002, Report of the National Astronomical Observatory of Japan, 6, 23
- Barkana, R. 1998, ApJ, 502, 531
- Becker, R. H., White, R. L., & Helfand, D. J. 1995, ApJ, 450, 559
- Borgeest, U., von Linde, J., & Refsdal, S. 1991, A&A, 251, L35
- Brotherton, M. S., Tran, H. D., Becker, R. H., Gregg, M. D., Laurent-Muehleisen, S. A., & White, R. L. 2001, ApJ, 546, 775
- Browne, I. W. A., et al. 2003, MNRAS, 341, 13
- Capelo, P. R., & Natarajan, P. 2007, astro-ph/0705.3042
- Cardelli, J. A., Clayton, G. C., & Mathis, J. S. 1989, ApJ, 345, 245
- Chelouche D., 2005, ApJ, 629, 667
- Cohn, J. D., Kochanek, C. S., McLeod, B. A., & Keeton, C. R. 2001, ApJ, 554, 1216
- Cutri, R. M., et al. 2003, The IRSA 2MASS All-Sky Point Source Catalog, NASA/IPAC Infrared Science Archive. <http://irsa.ipac.caltech.edu/applications/Gator/>,
- Elíasdóttir, Á., Hjorth, J., Toft, S., Burud, I., & Paraficz, D. 2006, ApJS, 166, 443
- Falco, E. E., et al. 1999, ApJ, 523, 617
- Gregg, M. D., Lacy, M., White, R. L., Glikman, E., Helfand, D., Becker, R. H., & Brotherton, M. S. 2002, ApJ, 564, 133
- Jackson, N., & Browne, I. W. A. 2007, MNRAS, 374, 168
- Johnston, D. E., et al. 2003, AJ, 126, 2281
- Kaiser, N., & Pan-STARRS Collaboration 2005, Bulletin of the American Astronomical Society, 37, 465
- Kassiola, A., & Kovner, I. 1993, ApJ, 417, 450
- Keller, S. C., et al. 2007, Publications of the Astronomical Society of Australia, 24, 1
- Kinney, A. L., Calzetti, D., Bohlin, R. C., McQuade, K., Storchi-Bergmann, T., & Schmitt, H. R. 1996, ApJ, 467, 38
- Kochanek, C. S. 1992, ApJ, 384, 1
- Kochanek, C. S., Falco, E. E., Schild, R., Dobrzycki, A., Engels, D., & Hagen, H.-J. 1997, ApJ, 479, 678
- Kochanek, C. S., Falco, E. E., & Muñoz, J. A. 1999, ApJ, 510, 590
- Kochanek, C. S., et al. 2000, ApJ, 543, 131
- Kochanek, C. S., Mochejska, B., Morgan, N. D., & Stanek, K. Z. 2006, ApJL, 637, L73
- Kochanek, C. S., Dai, X., Morgan, C., Morgan, N., Poindexter, S., & Chartas, G. 2006, ArXiv Astrophysics e-prints, arXiv:astro-ph/0609112
- Koopmans, L. V. E., & Treu, T. 2003, ApJ, 583, 606
- Lacy, M., Gregg, M., Becker, R. H., White, R. L., Glikman, E., Helfand, D., & Winn, J. N. 2002, AJ, 123, 2925
- Landolt, A. U. 1992, AJ, 104, 340
- Lawrence, A., et al. 2006, astro-ph/0604426
- Linder, E. V. 2004, PhRvD, 70, 043534
- Mannucci, F., Basile, F., Poggianti, B. M., Cimatti, A., Daddi, E., Pozzetti, L., & Vanzi, L. 2001, MNRAS, 326, 745
- Maoz, D., Bahcall, J. N., Doxsey, R., Schneider, D. P., Bahcall, N. A., Lahav, O., & Yanny, B. 1993, ApJ, 402, 69
- Menou, K., et al. 2001, ApJ, 561, 645
- Miyazaki, S., et al. 2002, PASJ, 54, 833
- Moro, D., & Munari, U. 2000, A&AS, 147, 361
- Mortonson, M. J., Schechter, P. L., & Wambsganss, J. 2005, ApJ, 628, 594
- Myers, S. T., et al. 2003, MNRAS, 341, 1
- Ofek, E. O., Rix, H.-W., Maoz, D., & Prada, F. 2002, MNRAS, 337, 1163

- Ofek, E. O., & Maoz, D. 2003, *ApJ*, 594, 101
- Ofek, E. O., Rix, H.-W., & Maoz, D. 2003, *MNRAS*, 343, 639
- Ofek, E. O., Maoz, D., Rix, H.-W., Kochanek, C. S., & Falco, E. E. 2006, *ApJ*, 641, 70
- Oguri, M. 2007, *ApJ*, 660, 1
- Oguri, M., et al. 2004, *PASJ*, 56, 399
- Oguri, M., et al. 2005, *ApJ*, 622, 106
- Oguri, M., et al. 2006, *AJ*, 132, 999
- Oke, J. B., et al. 1995, *PASP*, 107, 375
- Oscz, A., Serra-Ricart, M., Mediavilla, E., Buitrago, J., & Goicoechea, L. J. 1997, *ApJL*, 491, L7
- Peng, C. Y., Ho, L. C., Impey, C. D., & Rix, H.-W. 2002, *AJ*, 124, 266
- Pindor, B., et al. 2004, *AJ*, 127, 1318
- Poindexter, S., Morgan, N., Kochanek, C. S., & Falco, E. E. 2007, *ApJ*, 660, 146
- Reimers, D., Hagen, H.-J., Baade, R., Lopez, S., & Tytler, D. 2002, *A&A*, 382, L26
- Richards, G. T., et al. 2004, *AJ*, 127, 1305
- Rusin, D., Norbury, M., Biggs, A. D., Marlow, D. R., Jackson, N. J., Browne, I. W. A., Wilkinson, P. N., & Myers, S. T. 2002, *MNRAS*, 330, 205
- Rusin, D., & Kochanek, C. S. 2005, *ApJ*, 623, 666
- Schechter, P. L., & Wambsganss, J. 2002, *ApJ*, 580, 685
- Schlegel, D. J., Finkbeiner, D. P., & Davis, M. 1998, *ApJ*, 500, 525
- Schneider, D. P., et al. 2007, *AJ*, 134, 102
- Spergel, D. N., et al. 2007, *ApJS*, 170, 377
- Treu, T., & Koopmans, L. V. E. 2004, *ApJ*, 611, 739
- Treu, T., Koopmans, L. V., Bolton, A. S., Burles, S., & Moustakas, L. A. 2006, *ApJ*, 640, 662
- Turatto, M., Benetti, S., & Cappellaro, E. 2003, *From Twilight to Highlight: The Physics of Supernovae*, 200
- Tyson, A. 2005, *Observing Dark Energy*, 339, 95
- Vanden Berk, D. E., et al. 2001, *AJ*, 122, 549
- Wambsganss, J., Schmidt, R. W., Colley, W., Kundić, T., & Turner, E. L. 2000, *A&A*, 362, L37
- Wisotzki, L., Koehler, T., Kayser, R., & Reimers, D. 1993, *A&A*, 278, L15
- Wyithe, J. S. B., Winn, J. N., & Rusin, D. 2003, *ApJ*, 583, 58
- York, D. G., et al. 2000, *AJ*, 120, 1579